PROCEEDINGS OF SPIE

SPIEDigitalLibrary.org/conference-proceedings-of-spie

Ultrafast laser ablation of aqueous processed thick-film Li (Ni0.6Mn0.2Co0.2)O2 cathodes with 3D architectures for lithium-Ion batteries

Zhu, Penghui, Meyer, Alexandra, Pfleging, Wilhelm

Penghui Zhu, Alexandra Meyer, Wilhelm Pfleging, "Ultrafast laser ablation of aqueous processed thick-film Li(Ni0.6Mn0.2Co0.2)O2 cathodes with 3D architectures for lithium-Ion batteries," Proc. SPIE 11989, Laser-based Micro- and Nanoprocessing XVI, 119890F (4 March 2022); doi: 10.1117/12.2608609

SPIE.

Event: SPIE LASE, 2022, San Francisco, California, United States

Ultrafast laser ablation of aqueous processed thick-film $Li(Ni_{0.6}Mn_{0.2}Co_{0.2})O_2$ cathodes with 3D architectures for lithium-ion batteries

Penghui Zhu[a], Alexandra Meyer[a], Wilhelm Pfleging[a]
[a]Karlsruhe Institute of Technology (KIT), IAM-AWP, Hermann-von-Helmholtz-Platz 1, 76344 Eggenstein-Leopoldshafen, Germany

ABSTRACT

Lithium-ion batteries have dominated the field of electrochemical energy storage for years due to their high energy density. Recently, with the rapid development of E-mobility, the quest for high power and high energy batteries with reduced production costs has aroused great interest and is still a huge challenge. The energy density at battery level can be increased by using electrodes with thicknesses > 150 µm. However, capacity fade of thick-film electrodes at C-rates > C/2 is observed. To compensate the capacity loss, 3D architectures with a high aspect ratio are produced using ultrafast laser ablation. In addition, aqueous processing of cathodes using water-based binders can achieve environmentally friendly production and cost reduction by replacing the conventional organic PVDF binder and the toxic and volatile NMP solvent. However, the pH value of aqueous processed cathode slurries increases to 12 due to the reaction between active material and water, which decreases the specific capacity of the cells and on the other side results in chemical corrosion of the current collector during casting. In order to determine the optimal pH range and avoid the damage of the current collector, slurries with pH values ranging from 8 to 12 are manufactured.

In this work, thick-film $Li(Ni_{0.6}Mn_{0.2}Co_{0.2})O_2$ electrodes are manufactured with aqueous binders and acid adjustment, and are subsequently structured using ultrafast laser ablation. This combination is beneficial to achieve green production, low cost, high power, and high energy application of lithium-ion batteries.

Keywords: 3D battery, lase ablation, thick-film electrode, aqueous processing, NMC cathode, pH adjustment

1. INTRODUCTION

Lithium-ion batteries (LIBs) have been a great success in energy storage applications due to their high energy density, good safety, and long cyclic stability[1–4]. Besides, the specific energy of LIBs continues to grow at 6 %/year[5]. However, there are still many challenges waiting to be solved in order to make LIBs application in automotive industries competitive against conventional combustion engines. The production cost as well as energy density of LIBs are crucial factors that limit the widespread of application of LIBs in electric vehicles industries.

There are several approaches to reduce the battery production cost. The first method is to apply water-based binder instead of the state-of-the-art polyvinylidenfluoride (PVDF) binder. PVDF must be dissolved in the solvent N-methyl-pyrrolidone (NMP), which is expensive and highly toxic. Therefore, safety precautions such as ventilation and filtration devices are required for the protection of worker's safety[6]. Aqueous binders such as sodium carboxymethyl cellulose (Na-CMC) and styrene butadiene rubber (SBR) are environmentally benign and have only about 1/10 costs compared to PVDF[7]. Besides, during drying process, the removal of water solvent from electrode is 4.5 times faster than NMP solvent and the energy consumption can be reduced by 1/10 for the processing[8]. Aqueous binders have already been successfully used for the production of graphite anodes with / without silicon[9–11], while numerous researchers have reported the development of aqueous processing of cathode materials, such as $Li(Ni_{1/3}Mn_{1/3}Co_{1/3})O_2$ (NMC 111)[12, 13], $Li(Ni_{0.4}Mn_{0.4}Co_{0.2})O_2$ (NMC 442)[14], $Li(Ni_{0.5}Mn_{0.3}Co_{0.2})O_2$ (NMC 532)[15], and $LiFePO_4$[16]. However, the transition metal and lithium-ions leaching from active materials into water results in an increasing slurry pH value above 12[17]. This leads to general corrosion and pitting between alkaline slurry and aluminum current collector[18]. These major challenges hinder the further application of aqueous processing of cathodes.

With increasing electrode film thickness, the areal capacity of electrodes can be increased. Besides, the proportion of inactive materials such as current collector, separator in batteries will be reduced. Besides, the costs with regard to battery manufacturing such as cutting, stacking, and welding, will be lower[6]. However, the lithium-ion diffusion kinetics is limited in thick-film electrodes and thus leads to deterioration of electrochemical performance such as poor capacity retention

Laser-based Micro- and Nanoprocessing XVI, edited by Akira Watanabe, Rainer Kling, Proc. of SPIE Vol. 11989, 119890F · © 2022 SPIE
0277-786X · doi: 10.1117/12.2608609

with low power capability[19]. 3D battery concept provides new solution to this problem. With the combination of thick-film electrode and ultrafast laser ablation, the overall tortuosity inside electrode is reduced and the energy density as well as power density can be increased simultaneously[20–23].

In this work, we present the study of aqueous processed thick-film $Li(Ni_{0.6}Mn_{0.2}Co_{0.2})O_2$ (NMC 622) electrodes with pH adjustment using acetic acid. Laser ablation was applied to achieve line structures in thick-film electrodes (3D battery). The electrochemical performance of cells containing cathodes with different slurry pH values and with laser ablation was analyzed using rate capability analysis as well as cyclic voltammetry.

2. EXPERIMENTAL

2.1 Preparation of thick-film NMC cathodes

Commercially available NMC 622 powder (BASF SE, Germany) with a median particle size of 8.7 µm was used as active material, while carbon black (C-NERGY Super C65, Imerys G & C Belgium, Belgium) was applied as conductive additive. Water-based fluorine acrylic latex binder (TRD 202A, JSR Micro NV, Belgium) as well as Na-CMC (CRT 2000PA, Doe Wolff Cellulosic, Germany) with a substitution degree of 0.82 – 0.95 were used as binders for aqueous processed NMC 622 cathodes. NMC 622, carbon black, and deionized water were added into the premixed CMC solution and the cathode slurries were mixed in a dissolver (CDS, VMA-Getzmann, Germany) under vacuum (-1.0 bar) using 2000 rpm rotation speed for 20 min. After that, acetic acid was added in order to adjust the slurry pH value. The slurry was then mixed for 90 min under ambient condition using the same rotation speed. Finally, the shear sensitive binder TRD 202A was added to the slurry and was stirred with 500 rpm for 3 min. The pH value was measured 10 min after the mixing procedure was finished via a pH-meter (FE30-basic FiveEasy, Mettler-Toledo GmbH, Germany).

The slurry was deposited onto an aluminum-foil (thickness: 20 µm) with a doctor blade (ZUA 2000.100, Proceq, Switzerland) on a tape casting coater (MSK-AFA-L800-LD, MTI Corporation, USA). The coating speed was set at 5 mm/s and the electrode thickness was controlled by varying the gap of the doctor blade. Afterwards, the electrode was dried at room temperature to alleviate the chemical corrosion, which occurs at elevated temperatures. The thicknesses of dried electrodes were kept 190 - 240 µm to achieve thick-film electrodes with mass loading of 37 – 48 mg/cm^2. Finally, the dried cathodes were calendered using an electric rolling presser (MSK-2150, MTI Corporation, USA) with a constant calendering speed of 35 mm/s, in order to adjust the cathode porosity to 35 %. The electrode porosity was calculated based on the density and weight of each component. This method has been illustrated in our previous work[23].

2.2 Ultrafast laser ablation of NMC cathodes

Ultrafast femtosecond (fs) fiber laser (Tangerine, Amplitude Systèmes, France) with 380 fs pulse duration and a wavelength of 515 nm ($M^2 < 1.2$) was used to achieve line structures with 200 µm pitch in thick-film electrodes. The number of scans was varied from 30 to 50 according to the cathode film thickness, in order to ensure ablation depths down to the current collector. The laser scanning speed was 500 mm/s, while a repetition rate of 500 kHz and 4.3 W laser power were applied. After laser ablation, the electrodes were cut in circles with 12 mm in diameter for coin cell CR2032 design. The laser processing was performed in ambient air.

2.3 Cell assembly and electrochemical analysis

Before cell assembly, the NMC 622 cathodes were dried at a temperature of 130 °C for 24 h in a vacuum oven (VT 6025, Thermo Scientific, Germany). The NMC 622 cathodes were then stored in an argon-filled glove box (LABmaster pro, M. Braun, Germany) with $H_2O < 0.1$ ppm and $O_2 < 0.1$ ppm and were assembled versus lithium foil (0.25 mm thickness, Merck KGaA, Germany) in coin cells CR2032. Polypropylene separator (Celgard, USA) with a thickness of 25 µm and a diameter of 15 mm was used. A total amount of 120 µL electrolyte, which consists of ethylene carbonate and ethyl methyl carbonate (EC / EMC 3:7, wt.%) with 1.3 M hexafluorophosphate ($LiPF_6$) as conducting salt and 5 wt.% fluoroethylene carbonate (FEC) as additive, was added to each cell. All cell components were pressed and sealed using an electric crimper (MSK-160D, MTI Corporation, USA).

"Constant current - constant voltage" (CCCV) method was applied for rate capability analysis using a battery cycling system (BT 2000, Arbin Instruments, USA). At first, 3 cycles at C/20 were applied during the formation step, followed by C-rates from C/10 to 2C. C/10 and C/5 were performed for 5 cycles, while the other C-rates were carried out for 10 cycles. A specific capacity of 155 mAh/g and 1C = 0.99 h^{-1} were applied for the calculation of charge / discharge current at

different C-rates. For rate capability analysis, the voltage window was set to 3.0 – 4.2 V. As for cyclic voltammetry (CV), the lower and upper cut-off voltage were 3.0 and 4.3 V, while a scan rate of 0.02 mV/s was applied.

3. RESULTS AND DISCUSSION

3.1 Characterization of electrodes with pH adjustment

Slurries with different pH values were tape cast on aluminum foil and afterwards dried in ambient air without heating. The thickness, porosity, and mass loading of NMC 622 cathodes are summarized in Table 1. The slurry pH value increases to 12 without pH adjustment, which is similar to published results[13, 24]. This could be explained with the Li^+/H^+ exchange mechanism between NMC materials and water, which leads to the formation of products such as lithium hydroxide (LiOH), $LiHCO_3$, and Li_2CO_3 [25]. The porosity of dried electrode remains at 57 % after calendering process, suggesting the existence of many cavities inside the electrode. This has been verified by cross-sectional analysis shown in our previous work[26]: Cavities with diameters ranging from 60 to 290 µm are formed inside dried electrodes due to the hydrogen gas evolution. Besides, despite the highest film thickness of the electrode with slurry pH value 12 (thickness: 240 µm), its mass loading is only 36.9 mg/cm^2, which is about 10 mg/cm^2 less compared to other electrodes with pH adjustment. Therefore, pH adjustment is necessary for the aqueous processing of NMC cathodes to achieve a high energy density.

Table 1. NMC 622 electrodes after calendaring.

Slurry pH value	Film thickness (µm)	Porosity (%)	Mass loading (mg/cm^2)
12.1	240	57.5	36.9
10.0	200	34.6	47.4
9.0	189	35.1	44.2
8.4	191	31.7	47.1

In order to observe the aluminum surface which is in contact to slurry, the cathodes were soaked in deionized water and were washed with an ultrasonic cleaner device for 30 min. After the cathode films were removed, the aluminum foils were dried and characterized via scanning electron microscope (SEM, Phenom XL, Thermo Fisher Scientific, Netherlands), as shown in Figure 1. The corrosion and pitting occurred at the surface of aluminum current collector correspond to the cavities observed in the cathode film. For the thick-film electrode with slurry pH = 12, the extent of surface corrosion and pit formation is the most severe. The craters owing to the corrosion have diameters varying from 8 to 15 µm and small corrosion pits are built around the corrosion craters. With decreasing slurry pH values, the corrosion and pitting are alleviated. Besides, the slurry viscosity increases from 2 to 9 Pa·s at a reference shear rate of 50 s^{-1} with decreasing slurry pH from 12 to 8[26]. High slurry viscosity is conducive to limit the sedimentation of active material particles, binder migration, and convection of conductive agent[27]. Thus, acid addition can not only prevent the corrosion of aluminum current collector but is also beneficial for the thick-film manufacturing.

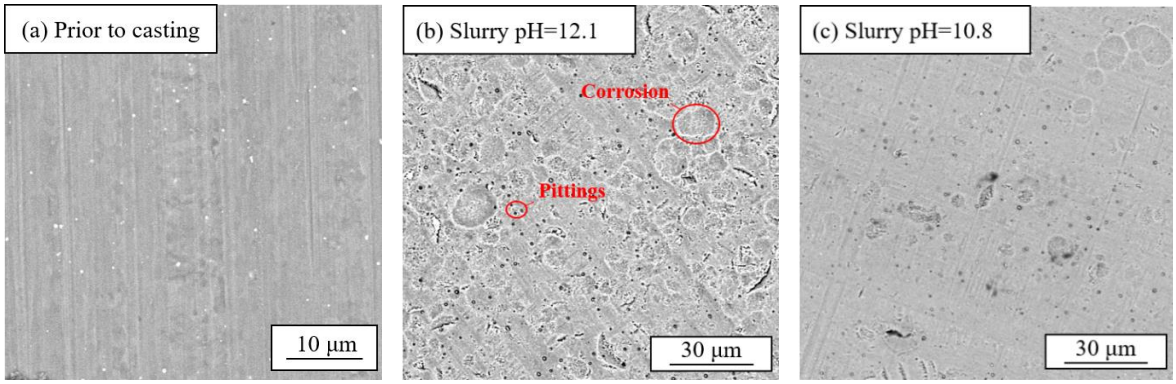

Figure 1. SEM images of aluminum foils (a) prior to casting and after the removal of the electrode film with slurry pH value of 12.1 (b) and 10.8 (c).

3.2 Laser ablation of NMC 622 electrodes

Thick-film electrodes deposited with slurry pH values of 12.1, 10.0, and 9.0 are subsequently calendered and structured using ultrafast fs-laser ablation. Line structures with 200 µm pitch are generated without damaging the current collector, as shown in Figure 2. A top width of 30 µm and a half-peak-width of 10 µm are achieved. The laser fluence is 15 J/cm^2, while a pulse overlap of 97 % is applied. The active mass loss due to laser ablation is 3 % to 10 %. No obvious debris formation is observed on the electrode surface or inside the channel structures (Figure 2). However, due to the existence of cavities and the inhomogeneity in film thickness, the laser ablation rate is different for cathode without acid addition. This causes the damage to the aluminum current collector or local drilling through the complete electrode. Thus, pH adjustment is necessary to meet the precondition of a reliable laser ablation.

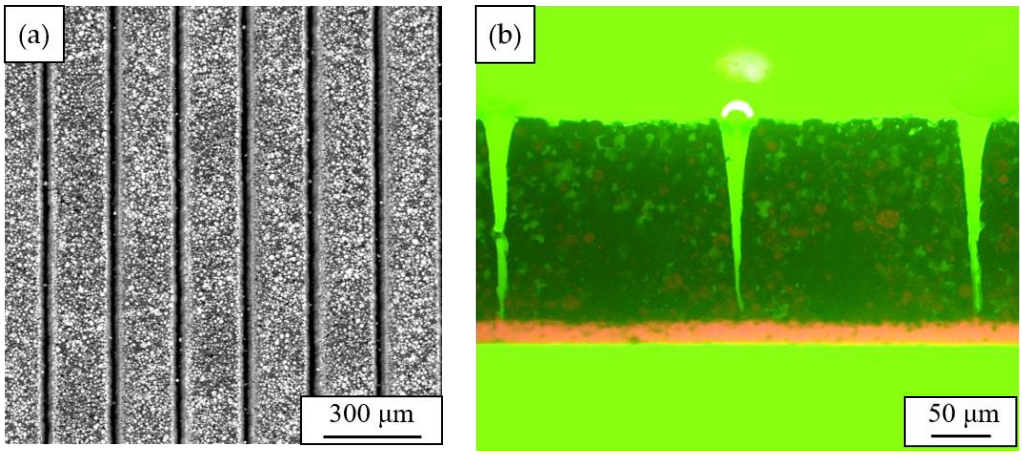

Figure 2. Laser structured NMC 622 cathode. (a) SEM image and (b) cross-sectional view of laser ablated thick-film NMC 622 cathode deposited with a slurry pH = 9.0.

3.3 Electrochemical performance of cells

Figure 3-a displays the CV measurement of cells containing unstructured NMC 622 cathodes deposited with different slurry pH values. Only one current peak appears during charge / discharge, which corresponds to redox reactions of Ni^{2+} / Ni^{4+} [28]. This implies that the addition of acetic acid does not affect the electrochemical reaction of NMC 622. The voltage differences between oxidation and reduction peaks (ΔE_p) are summarized in Table 2. It is observed that the voltage difference of redox peaks increases with decreasing slurry pH values, which indicates a higher barrier of electron transfer and a sluggish electrochemical reaction[29]. This is similar to the rate capability analysis, where the cells show lower capacity at C/5 to 1C with decreasing slurry pH value (high amount of acid addition). In electrodes without acid addition, the contact surface between electrode material and electrolyte is enlarged due to the increased size and number of cavities. Thus, the charge transfer resistance could be reduced and the diffusion kinetics of lithium-ions is improved.

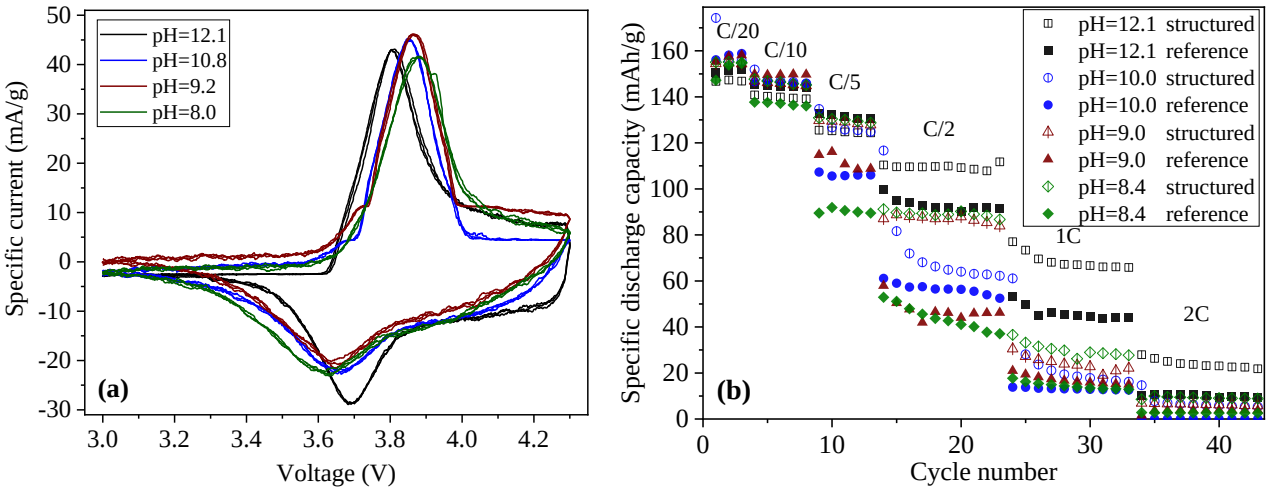

Figure 3. Electrochemical performance of cells with NMC 622 cathodes. (a) CV plots and (b) rate capability test of cells containing NMC 622 cathodes deposited with different slurry pH values.

Figure 3-b shows the specific discharge capacity of cells containing aqueous processed NMC 622 cathodes. During the formation step at C/20, the capacities are slightly increased. For example, for cells containing NMC 622 electrodes deposited with slurry pH values of 10 and 9, the specific capacity increases from 153 mAh/g to 158 mAh/g. This could be explained by the cation exchange on the surface of the active material, since a part of protons in the surface of NMC 622 can be swapped with lithium-ions from the electrolyte upon the first 3 cycles at C/20. At C/10, the electrode deposited with slurry pH 9.0 shows the highest capacity of 150 mAh/g, while the electrode deposited with slurry pH 8.4 shows the lowest capacity of 138 mAh/g. The cells with structured electrodes show the same or lower capacity in comparison to cells with unstructured electrodes. This might be due to the formation of solid electrolyte interface (SEI) between electrode and electrolyte[30]. The increased electrode surface owing to laser ablation results in the formation of a large reaction layer, which consumes a higher amount of electrolyte and active material. As the C-rate increases to C/5 and C/2, the cell containing electrode deposited with slurry pH = 12.1 maintains the highest capacity of 131 mAh/g and 93 mAh/g at C/5 and C/2, respectively, while the lowest specific capacities (90 mAh/g at C/5 and 43 mAh/g at C/2) belong to the cell containing electrode deposited with slurry pH 8.4. At C/5, all cells with structured cathode achieve the same capacity of 130 mAh/g as the cell with unstructured cathode without pH adjustment. With laser ablation, the discharge capacities of cells containing electrodes deposited with slurry pH 9 and 10 increase by 19 – 23 mAh/g at C/5. However, the advantage of laser ablation for the cathode without pH adjustment is not obvious for C-rates < C/2, this may be due to the high porosity of these cathode (> 50 %) compared to other electrodes with acid (35 %). When the C-rate is higher than C/2, laser structuring is feasible to further increase the capacity of cell containing NMC 622 cathode without acid addition. It could be due to the connection of cavities inside the electrode, which leads to increased number of diffusion pathways of lithium-ions from electrolyte to the electrode. At 1C and 2C, over 80 % capacity loss for all cells with thick-film electrodes is observed in comparison to the first cycles at C/20, except the cell containing structured electrode deposited without acid addition, showing the highest capacity of 68 mAh/h at 1C and 23 mAh/g at 2C.

Table 2. The voltage difference between redox peaks in CV measurement.

Slurry pH value	Voltage of oxidation peak (V)	Voltage of reduction peak (V)	Voltage difference ΔE_p (V)
12.1	3.80	3.69	0.11
10.8	3.86	3.66	0.20
9.2	3.87	3.64	0.23
8.0	3.88	3.63	0.25

4. CONCLUSIONS

CMC and TRD 202A were applied for the aqueous processing of NMC 622 slurry, while acetic acid was used to adjust the slurry pH value. Less corrosion and pitting is observed on the aluminum current collector with decreasing slurry pH value. Afterwards, the dried electrodes were structured using ultrafast laser ablation. Rate capability analysis shows a strong impact of the slurry pH value on the discharge capacity. At C-rates above C/10, the specific discharge capacity of the cell containing an electrode deposited with lower slurry pH value is decreased, while the electrode without acid addition shows the highest capacity. However, due to the existence of cavities, the porosity of this electrode is 20 % higher compared to others. This will lead to a decreased energy density. Laser ablation is feasible to increase the rate capability of cells with aqueous processed electrodes despite different slurry pH values, especially at discharge rates above C/5. Besides, unlike the cathode without acid addition, laser ablation provides controllable and precise structures in electrode. With enlarged surface between active materials and electrolyte, new lithium-ions diffusion pathways are generated. Considering the corrosion of current collector, energy density, the stability of electrodes, and the electrochemical performance, the slurry pH values should be adjusted to $9-10$ to balance the above-mentioned requirements and to meet a reliable precondition for laser ablation.

5. ACKNOWLEDGMENT

We are grateful to the help of our colleagues A. Reif, H. Besser, and Y. Zheng for their technical support in laser processing and material characterization. This research was funded by Federal Ministry of Education and Research (BMBF), project NextGen-3DBat, project No. 03XP01798F. In addition, we like to acknowledge equipment support in slurry mixing from Dr. W. Bauer and Dr. U. Kaufmann.

REFERENCES

[1] Goodenough, J. B. and Park, K.-S., "The Li-ion rechargeable battery: a perspective," Journal of the American Chemical Society 135(4), 1167–1176 (2013).

[2] Kwade, A., Haselrieder, W., Leithoff, R., Modlinger, A., Dietrich, F. and Droeder, K., "Current status and challenges for automotive battery production technologies," Nature Energy 3(4), 290–300 (2018).

[3] Blomgren, G. E., "The development and future of lithium ion batteries," Journal of The Electrochemical Society 164(1), A5019 (2016).

[4] Nitta, N., Wu, F., Lee, J. T. and Yushin, G., "Li-ion battery materials: present and future," Materials today 18(5), 252–264 (2015).

[5] Pistoia, G. and Liaw, B., [Behaviour of lithium-ion batteries in electric vehicles: battery health, performance, safety, and cost], Springer (2018).

[6] Wood III, D. L., Li, J. and Daniel, C., "Prospects for reducing the processing cost of lithium ion batteries," Journal of Power Sources 275, 234–242 (2015).

[7] Kim, G. T., Jeong, S. S., Joost, M., Rocca, E., Winter, M., Passerini, S. and Balducci, A., "Use of natural binders and ionic liquid electrolytes for greener and safer lithium-ion batteries," Journal of Power Sources 196(4), 2187–2194 (2011).

[8] Susarla, N., Ahmed, S. and Dees, D. W., "Modeling and analysis of solvent removal during Li-ion battery electrode drying," Journal of Power Sources 378, 660–670 (2018).

[9] Ling, M., Qiu, J., Li, S., Zhao, H., Liu, G. and Zhang, S., "An environmentally benign LIB fabrication process using a low cost, water soluble and efficient binder," Journal of Materials Chemistry A 1(38), 11543–11547 (2013).

[10] Zheng, Y., Seifert, H. J., Shi, H., Zhang, Y., Kübel, C. and Pfleging, W., "3D silicon/graphite composite electrodes for high-energy lithium-ion batteries," Electrochimica Acta 317, 502–508 (2019).

[11] Meyer, A., Ball, F. and Pfleging, W., "The Effect of Silicon Grade and Electrode Architecture on the Performance of Advanced Anodes for Next Generation Lithium-Ion Cells," Nanomaterials 11(12) (2021).

[12] Çetinel, F. A. and Bauer, W., "Processing of water-based $LiNi_{1/3}Mn_{1/3}Co_{1/3}O_2$ pastes for manufacturing lithium ion battery cathodes," Bulletin of Materials Science 37(7), 1685–1690 (2014).

[13] Bauer, W., Çetinel, F. A., Müller, M. and Kaufmann, U., "Effects of pH control by acid addition at the aqueous processing of cathodes for lithium ion batteries," Electrochimica Acta 317, 112–119 (2019).

[14] Chen, Z., Kim, G.-T., Chao, D., Loeffler, N., Copley, M., Lin, J., Shen, Z. and Passerini, S., "Toward greener lithium-ion batteries: Aqueous binder-based $LiNi_{0.4}Co_{0.2}Mn_{0.4}O_2$ cathode material with superior electrochemical performance," Journal of Power Sources 372, 180–187 (2017).

[15] Bichon, M., Sotta, D., Dupré, N., Vito, E. de, Boulineau, A., Porcher, W. and Lestriez, B., "Study of immersion of $LiNi_{0.5}Mn_{0.3}Co_{0.2}O_2$ material in water for aqueous processing of positive electrode for Li-ion batteries," ACS applied materials & interfaces 11(20), 18331–18341 (2019).
[16] Li, J., Armstrong, B. L., Kiggans, J., Daniel, C. and Wood III, D. L., "Lithium ion cell performance enhancement using aqueous $LiFePO_4$ cathode dispersions and polyethyleneimine dispersant," Journal of The Electrochemical Society 160(2), A201 (2012).
[17] W. Blake Hawley, Anand Parejiya, Yaocai Bai, Harry M. Meyer, David L. Wood and Jianlin Li, "Lithium and transition metal dissolution due to aqueous processing in lithium-ion battery cathode active materials," Journal of Power Sources 466, 228315 (2020).
[18] Church, B. C., Kaminski, D. T. and Jiang, J., "Corrosion of aluminum electrodes in aqueous slurries for lithium-ion batteries," J Mater Sci 49(8), 3234–3241 (2014).
[19] Park, K.-Y., Park, J.-W., Seong, W. M., Yoon, K., Hwang, T.-H., Ko, K.-H., Han, J.-H., Jaedong, Y. and Kang, K., "Understanding capacity fading mechanism of thick electrodes for lithium-ion rechargeable batteries," Journal of Power Sources 468, 228369 (2020).
[20] Pfleging, W., "A review of laser electrode processing for development and manufacturing of lithium-ion batteries," Nanophotonics 7(3), 549–573 (2018).
[21] Pfleging, W., "Recent progress in laser texturing of battery materials: a review of tuning electrochemical performances, related material development, and prospects for large-scale manufacturing," International Journal of Extreme Manufacturing (2020).
[22] Park, J., Hyeon, S., Jeong, S. and Kim, H.-J., "Performance enhancement of Li-ion battery by laser structuring of thick electrode with low porosity," Journal of Industrial and Engineering Chemistry 70, 178–185 (2019).
[23] Zhu, P., Seifert, H. J. and Pfleging, W., "The ultrafast laser ablation of $Li(Ni_{0.6}Mn_{0.2}Co_{0.2})O_2$ electrodes with high mass loading," Applied Sciences 9(19), 4067 (2019).
[24] Wood, M., Li, J., Ruther, R. E., Du, Z., Self, E. C., Meyer III, H. M., Daniel, C., Belharouak, I. and Wood III, D. L., "Chemical stability and long-term cell performance of low-cobalt, Ni-Rich cathodes prepared by aqueous processing for high-energy Li-Ion batteries," Energy Storage Materials 24, 188–197 (2020).
[25] Shkrob, I. A., Gilbert, J. A., Phillips, P. J., Klie, R., Haasch, R. T., Bareño, J. and Abraham, D. P., "Chemical weathering of layered Ni-rich oxide electrode materials: evidence for cation exchange," Journal of The Electrochemical Society 164(7), A1489 (2017).
[26] Zhu, P., Han, J. and Pfleging, W., "Characterization and Laser Structuring of Aqueous Processed $Li(Ni_{0.6}Mn_{0.2}Co_{0.2})O_2$ Thick-Film Cathodes for Lithium-Ion Batteries," Nanomaterials 11(7), 1840 (2021).
[27] Hawley, W. B. and Li, J., "Electrode manufacturing for lithium-ion batteries—Analysis of current and next generation processing," Journal of Energy Storage 25, 100862 (2019).
[28] Shaju, K. M., Rao, G. S. and Chowdari, B. V.R., "Performance of layered Li $(Ni_{1/3}Co_{1/3}Mn_{1/3})O_2$ as cathode for Li-ion batteries," Electrochimica Acta 48(2), 145–151 (2002).
[29] Elgrishi, N., Rountree, K. J., McCarthy, B. D., Rountree, E. S., Eisenhart, T. T. and Dempsey, J. L., "A practical beginner's guide to cyclic voltammetry," Journal of chemical education 95(2), 197–206 (2018).
[30] Peled, E., "The electrochemical behavior of alkali and alkaline earth metals in nonaqueous battery systems—the solid electrolyte interphase model," Journal of The Electrochemical Society 126(12), 2047 (1979).